https://doi.org/10.1016/j.jpowsour.2020.227856
This is the Pre-Published Version.

Achieving a stable zinc electrode with ultralong cycle life by implementing a flowing electrolyte

Wentao Yu[a], Wenxu Shang[a], Xu Xiao[a], Peng Tan[a*], Bin Chen[b], Zhen Wu[c,d], Haoran Xu[d], Meng Ni[d,e*]

[a.] Department of Thermal Science and Energy Engineering, University of Science and Technology of China (USTC), Hefei 230026, Anhui, China.
[b.] Institute of Deep Earth Sciences and Green Energy, Shenzhen University, Shenzhen, 518060, China.
[c.] Shaanxi Key Laboratory of Energy Chemical Process Intensification, School of Chemical Engineering and Technology, Xi'an Jiaotong University, Xi'an, 710049, Shaanxi, China.
[d.] Department of Building and Real Estate, The Hong Kong Polytechnic University, Hung Hom, Kowloon, Hong Kong, China.
[e.] Environmental Energy Research Group, Research Institute for Sustainable Urban Development (RISUD), The Hong Kong Polytechnic University, Hung Hom, Kowloon, Hong Kong, China.

* Corresponding authors:
Email: pengtan@ustc.edu.cn (Peng Tan)
Email: meng.ni@polyu.edu.hk (Meng Ni)

Abstract: Zinc electrode stability is one of the major problems that restrict the wide application of secondary zinc-based batteries. In this work, the impacts of flowing electrolyte on the suppression of zinc dendrite are systematically investigated through experimental and numerical investigations. In a static electrolyte condition, the stability of the zinc electrode increases with an increase of the applied current density. In the presence of flowing electrolyte, the lifespan of the zinc electrode at the current density of 10 mA cm^{-2} increases dramatically from 900 cycles in the static electrolyte to 2580 cycles with a flow rate of 30 rad min^{-1}, and further increases to 4725 cycles when increasing the flow rate to 50 rad min^{-1}. Moreover, by changing the inlet flow direction from the side to the bottom, a more stable electrode with the lifespan of

© 2020. This manuscript version is made available under the CC-BY-NC-ND 4.0 license http://creativecommons.org/licenses/by-nc-nd/4.0/

18000 cycles (1200 h) is achieved. The numerical calculation illustrates that the distribution of zincate ions is more uniform in the presence of the flowing electrolyte, which is the key to the dendrite suppression. Thus, with the implementation of flowing electrolyte, a stable zinc electrode with an ultralong lifespan is demonstrated, which is promising for practical applications.

Keywords: Zinc electrode; dendrite; symmetric battery; flowing electrolyte; cycling stability.

1. Introduction

With the increasing demands for electrochemical energy storage, zinc-based batteries (e.g., Zn-MnO_2, Zn-Ni, Zn-Ag, Zn-Co, and Zn-air) have demonstrated the potential as power sources ranging from portable electronic devices to large-scale energy storage due to the relatively low price and safety [1–9]. Zinc metal is considered to be one of the ideal negative electrode materials for its instinct properties [10]. Firstly, zinc is one of the most abundant elements on the earth and is easy to obtain, leading to a low price. Secondly, zinc has a high theoretical capacity of 820 mAh g^{-1}, which is far higher than the electrode materials of lithium-ion batteries [11]. Thirdly, the commonly used electrolytes in zinc-based batteries are non-flammable and non-toxic aqueous solutions, which dramatically improves the safety and application ranges [10]. Despite of the aforementioned advantages, the poor long-term operational stability of the zinc electrode is still the major obstacle that limits the application of secondary zinc-based batteries [12].

Passivation, dendrites, and hydrogen evaluation are currently the major issues in

the zinc electrode [13]. Passivation is mainly caused by insoluble and insulating products and by-products in alkaline solutions [14]. During the oxidation of the zinc electrode, the electrochemical reaction product is zincate ions, which can be reduced to zinc metal in the charge process. However, when the local concentration of zincate ions reaches the saturated value, zinc oxide will precipitate out of solution and adhere to the electrode surface. Due to the insoluble property of zinc oxide, the active reaction surface area gradually shrinks with the deposition of zinc oxide, deteriorating the battery performance. Hydrogen evolution reaction (HER) is a parasitic reaction as the zinc electrode potential is more negative than that of the HER, which leads to the capacity deterioration and the utilization decay of the zinc electrode [13,15]. Comparatively, dendrite is a more severe problem that can result in the short-circuit in the long-term operation [16]. During charge, zincate ions are reduced and deposited on the zinc electrode. However, the concentrations of zincate ions in the electrode surface and the bulk electrolyte solution are usually different, which makes the zincate ions more likely to deposit on protrusions of the electrode surface [13]. As the charge and discharge cycles repeating, zinc dendrites will gradually form on the zinc electrode.

Zinc dendrites have been investigated for decades since the secondary zinc-based batteries were proposed. Many feasible strategies have been proposed to suppress the dendrite growth of the zinc electrode, such as the electrode designs, applying additives, and pulse charging protocols [13]. The works of electrode designs mainly focus on enlarging the zinc deposition surface and providing accommodation for

deposited zinc. Li et al. developed a neutral aqueous Zn/MnO_2 battery with a hybrid electrode by mixing zinc particles with activated carbon, which improved the capacity retention from 56.7% to 85.6% after 80 cycles [17]. Joseph et al. proposed a three-dimensional sponge zinc electrode for nickel-zinc alkaline batteries [18]. Wang et al. used conductive graphite fibers as the current collector and achieved 700 h lifespan in a symmetric battery [19]. However, with the cycles goes by, the zinc electrode shape change will damage the pristine structures and result in the decay of the zinc electrode stability and battery performance. Apart from the electrode designs, inorganic and organic additives are commonly used to suppress dendrite growth. Adler et al. found that fluoride and carbonate anions could effectively alleviate the shape change of zinc electrode and extend the battery lifespan from 100 cycles to 460 cycles [20]. Wang et al. added bismuth ion and tetrabutylammonium bromide to the alkaline solution and found the synergistic effect of bismuth ion and tetrabutylammonium bromide on suppressing the dendrite growth [21]. Kim et al. reported that zinc dendrite growth could be effectively suppressed with an increase content of SnO, but the deposited zinc became rough and crumbling electrodeposits when the pure Sn phase reached a relatively large amount [22]. As for organic additives, Zhu et al. reported that ionic types of perfluorosurfactants had a positive effect on the electrochemical behavior of zinc, and more compact and uniform deposited zinc was obtained in the presence of surfactants [23]. Lan et al. proposed tetra-alkyl ammonium hydroxides as effective additives for zinc dendrite inhibitor, which highly improved the stability of the zinc electrode [24]. Amir et al. tested the

effects of polyethyleneimine on zinc-ion batteries with a 0.5 M $ZnSO_4$ solution. The results elucidated that the morphology of the deposited zinc changed from laminated hexagonal large crystals to a compact layer without preferential growth morphology in the presence of polyethyleneimine, and the electrodeposition efficiency was apparently improved in 50 cycles [25]. However, the additives may have negative effects on the species transport and conductivity of the electrode and electrolyte. Pulse charging protocols mean that using a periodically changing current density to replace a constant current density during charge. When employing the pulsed charging protocols, the concentration of $Zn(OH)_4^{2-}$ at the zinc electrode surface is re-established after a short reduction period [26]. Garcia et al. investigated the pulsed charging protocols in a commercial nickel-zinc battery and found that the cycle life was improved from dozens of cycles to hundreds of cycles [26]. In spite of the promising effects on the dendrite inhibition, the pulsed large currents may do harm to the positive electrodes and bring about inconvenience for practical applications.

Besides these methods, applying flowing electrolyte has been considered as a promising strategy for improving the stability of the zinc electrode via changing the zincate ion concentration distribution and avoiding the accumulation of zincate ions [27–29]. Moreover, the passivation is alleviated at the same time by balancing the zincate ion concentration and bringing the by-products outside the electrolyte chamber. Zhang et al. reported that zinc dendrite growth was prevented on the cadmium substrate in a zinc-nickel battery with flowing electrolyte [30]. Wang et al. found that the flowing electrolyte changed the zincate ion distribution and contributed to a more

compact and uniform morphology [31]. However, this strategy has attracted little attention in the research of the zinc electrode. As far as we know, the reported works only focused on the comparison between the flowing electrolyte and the static electrolyte. A comprehensive investigation on the flowing electrolyte, such as the relationship between flow rates and battery operation, the impacts of flow orientation, has not been reported yet.

Herein, we provided a systematic investigation on the optimization of flowing electrolyte to achieve a highly stable zinc electrode. In the beginning, the dendrite formation under different current densities and capacities with a conventional static electrolyte was characterized. Then, the electrolyte flowed through the electrolyte chamber driven by a peristaltic pump, and the impacts of flow rates under different current densities were investigated. Finally, based on the aforementioned works, flow orientation was changed to further increase the stability of the zinc electrode. This work combines charge-discharge tests, characterization, and numerical simulations, and provides a reference for further development of durable zinc electrodes for advanced zinc batteries.

2. Methods

2.1 Experimental setup

With a focus on the stability of zinc electrodes, a symmetric structure composed of two zinc electrodes was used in this work. As shown in Fig. 1a, the main parts of the symmetric battery are two zinc electrodes, two current collectors, and an electrolyte chamber with a diameter of 10 mm and a width of 5 mm. Actually, this

structure has been widely used in zinc-based batteries by replacing one zinc electrode with other electrodes (e.g., air electrode) [32–35]. During discharge, zinc strips on one electrode while plates on the other electrode, and a converse process occurs during charge. As the operation continues, the plating/stripping process repeats and dendrites gradually form on both electrodes. When conducting the flow experiments, the segments were the same as the static ones except for replacing the electrolyte chamber with a new one containing electrolyte flows, as shown in Fig. 1b. A peristaltic pump was used to drive the flowing electrolyte and the rotating rate was used to represent the flow rate, in which the volume flow rate was proportional to the rotating rate, and 10 rad min^{-1} corresponded to the volume flow rate of 1.5 mL min^{-1}.

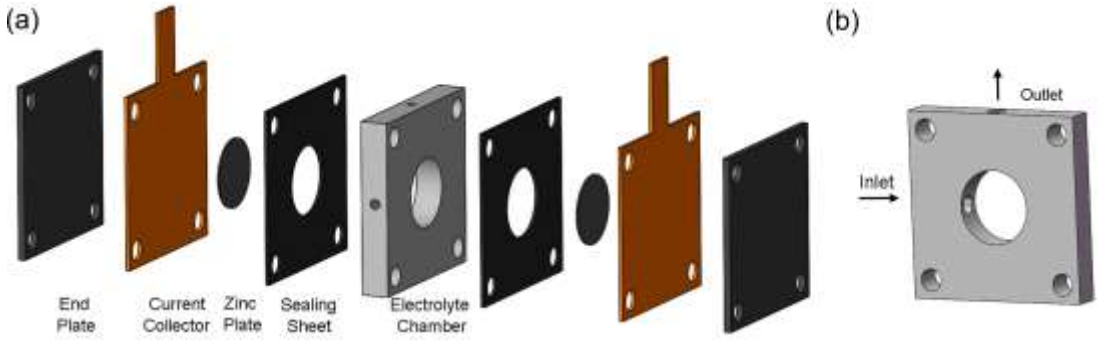

Fig. 1. (a) Schematic diagram of the symmetric zinc battery; (b) flow electrolyte chamber (with a diameter of 10 mm and a width of 5 mm).

Two zinc plates (purity> 99.99%) were used as the electrodes with a diameter of 10 mm and a thickness of 0.5 mm. An alkaline solution containing 6 M potassium hydroxide with 0.2 M zinc acetate was selected as the electrolyte. The total volume of the electrolyte in the tank was 40 mL in flow batteries. All experiments were conducted at room temperature.

2.2 Characterization

The lifespan of symmetric batteries was tested to evaluate the stability of the zinc electrode by Neware Battery System at constant current densities ranging from 1 to 15 mA cm^{-2}. The deposition and dissolution processes of zinc continued to take place on both electrodes at a constant current density until the short-circuit occurred. As shown in Fig. S1 in supplementary information (SI), the charge and discharge voltages dropped dramatically and maintained at a constant value. After the cycle lifespan test, the zinc electrodes were disassembled and rinsed in deionized water and then dried in a vacuum drying oven. The dendrite morphology was observed by a scanning electron microscope (Genimi SEM 500, 3.0 kV).

2.3 Numerical investigation

A three-dimensional model was built to further investigate the flow impacts on the zincate ion distribution in COMSOL. The geometrical structure of the three-dimensional computational domain is shown in Fig. S2 (SI). To simulate the generation and disappearance of zincate ions on both electrodes, two opposite zincate concentration fluxes were used to replace the electrochemical reaction for simplicity. The material balance is governed by the following species' equation:

$$\frac{\partial c_i}{\partial t} + \mathbf{u}\nabla c_i + \nabla(-D_i\nabla c_i - z_i\mu_i F c_i \nabla V) = R_i \quad (1)$$

where c_i represents the concentration of species i, $\mathbf{u}$ is the velocity of the flowing electrolyte, D_i, z_i, and μ_i are the diffusion coefficient, the charge number, and the mobility of species i, respectively. F is the Faraday constant, R_i is the reaction rate, and V is the battery potential. Incompressible Navier-Stokes equation is used to describe the

movement of the flowing electrolyte:

$$\rho\left(\frac{\partial \mathbf{u}}{\partial t}+\mathbf{u}\cdot\nabla\mathbf{u}\right)=-\nabla p+\mu\nabla^{2}\mathbf{u}+f \quad (2)$$

where ρ and μ are the density and viscosity of the flowing electrolyte, respectively; f stands for the external force, and p is the pressure. The computation was implemented under isothermal conditions. The parameter values used in the model are listed in Table S1 (SI), from which the laminar model was selected.

3. Results and discussion

3.1 Static conditions

The stability of zinc electrodes operated under static conditions was investigated to identify the factors that influence the zinc dendrite formation. Firstly, the cycle lifespan tests employing different capacities were performed at a constant current density of 10 mA cm^{-2}. To control different discharge capacities, the discharge time was set as 1, 2, 5, and 10 min, respectively. As shown in Fig. 2a and 2b, the cycle lifespan decreases dramatically with an increase of the capacity. At the discharge time of 1 min, the symmetric battery operates stably for about 189 h until the short-circuit occurs. However, the cycle life is only 21 h when increasing the capacity to ten times (discharge time of 10 min). For the symmetric structure, the overall concentration of zincate ions in the electrolyte maintained at a constant level. Therefore, only the local concentration changes under different discharge capacities. When employing a constant current density, the zincate concentration gradient around the zinc electrode increases with the time goes by, which makes it easier for the dendrite growth.

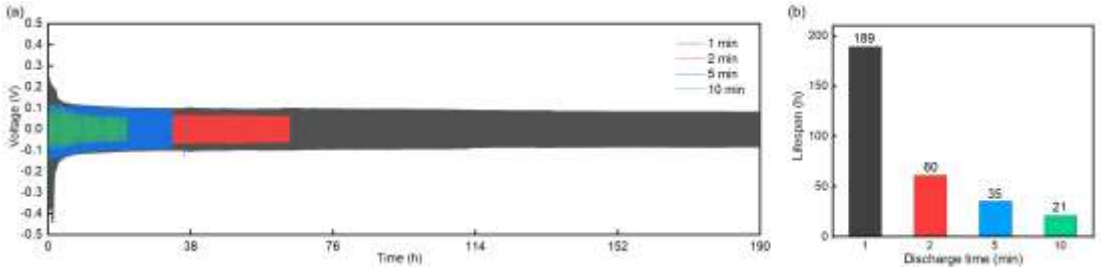

Fig. 2. (a) Charge-discharge cycle curves with different capacities; (b) Lifespan comparison between different capacities.

The influence of current density on the zinc electrode stability was also tested. To maintain the same capacity, the lifespan tests at a series of current densities of 1, 2.5, 5, 7.5, 10, and 15 mA cm^{-2} were performed at the corresponding time of 10 min, 4 min, 2 min, 1 min 20 s, 1 min, and 40 s. The single-cycle charge-discharge curves at different current densities are shown in Fig. S3 (SI). Obviously, the overpotential of the symmetric battery is positively related to the increment of the current density, which is caused by the concentration and ohmic polarization effects. Fig. 3 shows the charge-discharge voltage curves at different current densities. At a current density of 1 mA cm^{-2}, the symmetric battery operates stably for 89 h before getting short-circuit, while the lifespan increases to 250 h at the current density of 15 mA cm^{-2}. It is evident that the zinc electrode operated at higher current densities exhibits better cycle stability than that with a lower one.

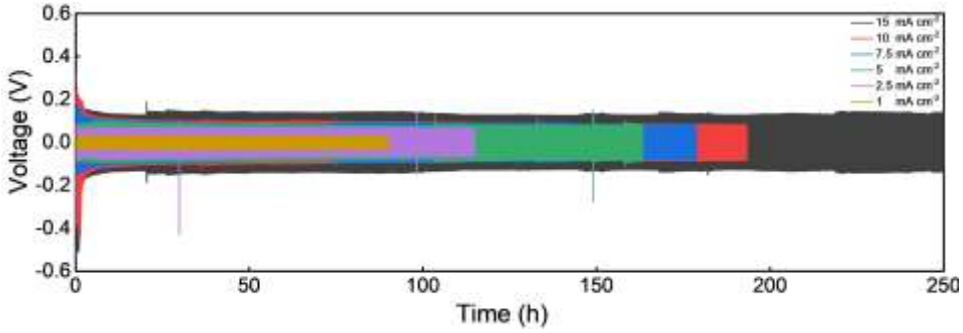

Fig. 3. Charge-discharge cycle curves at different current densities in a static electrolyte.

To further investigate the impact of current density on the zinc deposition, the ex-situ SEM was used to reveal the differences of micro-morphology of zinc dendrites at different current densities. Fig. 4a shows the zinc dendrite morphology at a current density of 1 mA cm^{-2}, from which the deposited zinc demonstrates an irregular porous structure. Fig. 4b shows the SEM image with the same magnification at the current density of 15 mA cm^{-2}. Conversely, the size of the deposited zinc was larger than that at 1 mA cm^{-2}. The results indicate that the deposited zinc has a more compact structure when operating at a higher current density. This is probably because that high current densities lead to high reaction rates on the electrode, accelerating the deposition process and decreasing the concentration gradient. Thus, the dendrite growth rate is relatively lower with a compact structure. During the long-term operation, this structure has a positive impact on the battery lifespan as the deposited zinc is not likely to detach from the electrode substrate, which improves the utilization rate of zinc and reduces the capacity attenuation.

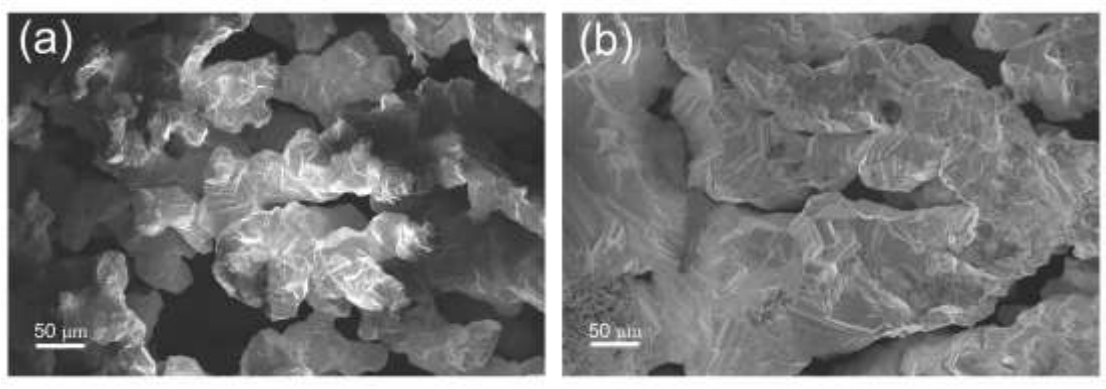

Fig. 4. Morphology of deposited zinc at different current densities: (a) 1 mA cm^{-2} and (b) 15 mA cm^{-2}.

3.2 Effects of flow rates

The flowing electrolyte was then introduced to the symmetric zinc battery. The single-cycle discharge-discharge voltage curves with different flow rates at high and low current densities are illustrated in Fig. S4 (SI). As shown in Fig. S4a (SI), at the current density of 1 mA cm^{-2}, the overpotentials show a downward trend with an increase of the flow rate. When increasing the current density to 10 mA cm^{-2}, this trend is more obvious, as shown in Fig. S4b (SI). The results indicate that the flowing electrolyte can decrease the overpotential of the zinc electrode, which may be attributed to the enhanced mass transfer due to convection.

After the single-cycle test, the lifespan test was conducted in different flow rate conditions. The experiments at a current density of 1 mA cm^{-2} and discharge time of 40 min were tested firstly, as shown in Fig. 5a. The lifespan of the symmetric batteries at the flow rates of 0, 10, 20, 30 rad min^{-1} is 57, 54, 111, and 1279 cycles, respectively. When employing a low flow rate, the lifespan does not change obviously. This is probably because the low flow rate contributes little to the local concentration of zincate ions. With an increase of the flow rate, the lifespan improves dramatically. Especially, when the flow rate is increased to 30 rad min^{-1}, the lifespan is approximately ten times than that of 20 rad min^{-1}. Fig. 5b shows the lifespan curves at a current density of 10 mA cm^{-2}. To maintain the same capacity, the discharge time was set as 2 min. The total lifespan is 900, 870, 2580, and 4725 cycles at the flow rates of 0, 10, 30, 50 rad min^{-1}. Similar to the situation at the low current density, the performance is apparently improved with a high flow rate. Besides, the cycle numbers

still precede the value at the low current density when exerting the same flow rate. At the same flow rate of 30 rad min^{-1}, the lifespan is improved by about 20 times (from 57 to 1279 cycles) compared with the static one at the current density of 1 mA cm^{-2}, while the amplitude is just about 3 times (from 900 to 2580 cycles) at the current density of 10 mA cm^{-2}. When further increasing the flow rate to 50 rad min^{-1}, the lifespan is increased to 4725 cycles. Thus, with an increase of the applied current density, a higher flow rate is needed to obtain more durable zinc electrodes.

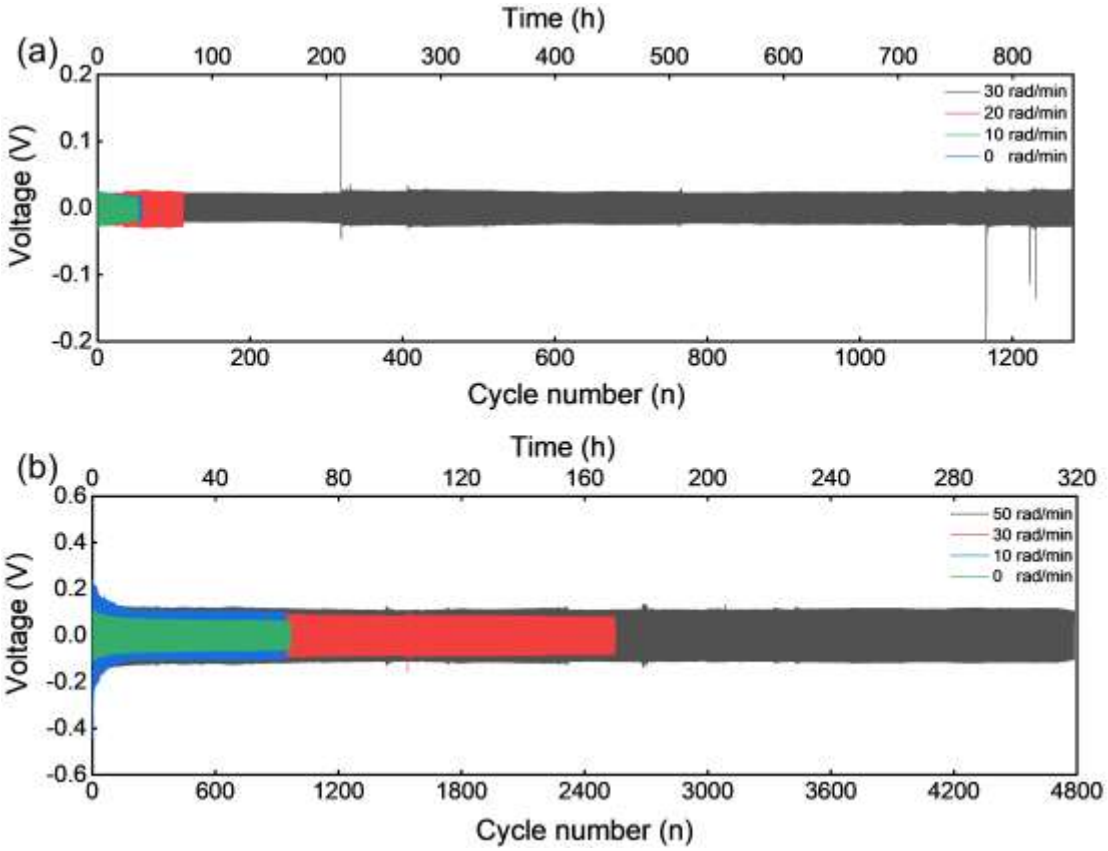

Fig. 5. Charge-discharge cycle curves with different flow rates: (a) 1 mA cm^{-2} and (b) 10 mA cm^{-2}.

The morphologies of deposited zinc under different flow rates were observed by SEM, as shown in Fig. 6. It is obvious that the surface of the deposited zinc becomes rougher with an increment of the flow rate, which indicates that zinc can uniformly

deposit on the whole surface rather than only on the protrusions of the electrode surface, forming a relatively compact film. As the zinc atom deposition is controlled by the thermodynamics and kinetics, the morphology of the deposited zinc is determined by the competition between the vertical growth and the horizontal growth [31]. When employing the flowing electrolyte, the deposited rate on the electrode surface can be well balanced, and thus the dendrite is effectively inhibited. Therefore, the stability of the zinc electrode is improved. This observation also explains the phenomenon that the lifespan improvement of flowing electrolyte at the low current density is more obvious. At the current density of 1 mA cm^{-2}, the deposited zinc with loose morphology is shaped by the flowing electrolyte and becomes more compact. Thus, the growth rate of the zinc dendrite is retarded due to the compact deposited zinc.

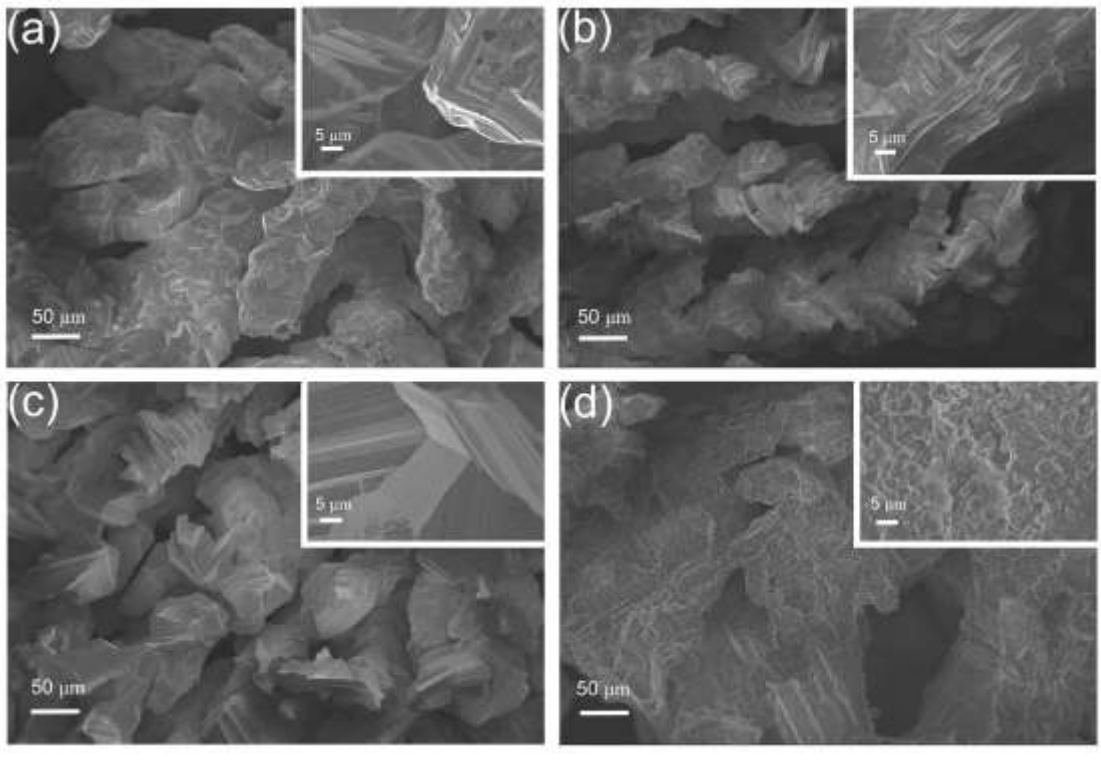

Fig. 6. Morphology of deposited zinc with different flow rates at a current density of 10 mA cm^{-2}:

(a) 0 rad min^{-1} (b) 10 rad min^{-1} (c) 30 rad min^{-1} (d) 50 rad min^{-1}.

3.3 Effects of flow orientation

After the symmetric batteries are short-circuited, the photographs of zinc electrodes in static and flow conditions are shown in Fig. S5 (SI). Apparently, in the static condition, the position of the dendrite is at the bottom of the zinc electrode, which is consistent with the previous reports [32]. In the flow condition, except for the bottom position, zinc is also deposited between the middle and the bottom of the electrode. As the short-circuit still occurs at the bottom of the electrode which indicates that the flowing electrolyte is not fully utilized, to further extend the lifespan of the zinc electrode, the inlet flow orientation was changed from the side to the bottom and the channel becomes direct, as shown in Fig. S6a (SI). The lifespan test was performed at 10 mA cm^{-2} with the flow rate of 30 rad min^{-1}, and one discharge-charge cycle time was set as 4 min. As illustrated in Fig. 7, after 18000 cycles (1200 h) the voltages are still stable without the occurrence of short-circuit, and this lifespan is surprisingly higher than that with the side channel (2580 cycles, 172 h). This cycling stability, to our best knowledge, is also one of the highest among literature [36–38]. Fig. S6b (SI) presents the zinc electrode image after the stability test. The deposited zinc evenly distributes on most surfaces of the electrode compared with the aforementioned results shown in Fig. S5 (SI).

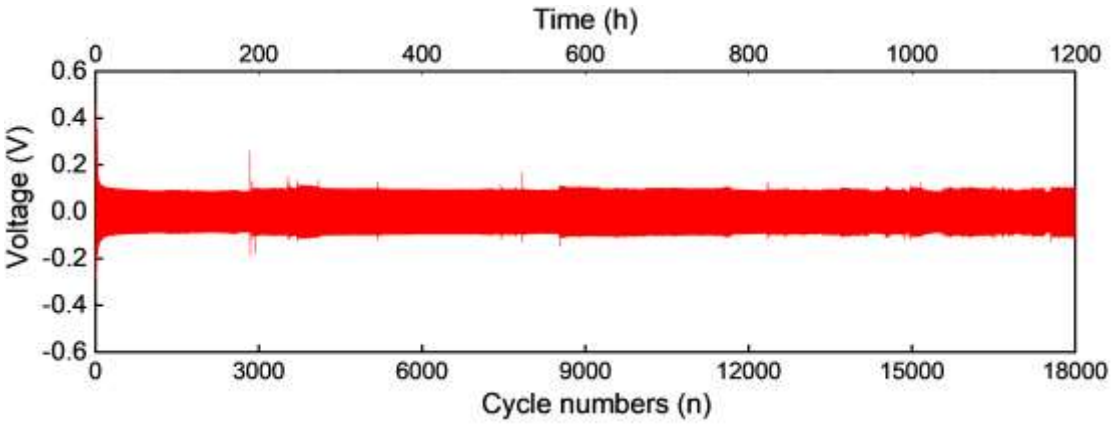

Fig. 7. Charge-discharge cycle curves with a direct flow channel.

To elucidate the intrinsic reason, a three-dimensional model was built to investigate the influence of the flow orientation on the concentration distribution. As shown in Fig. 8a, a visible concentration gradient exists in the static electrolyte. When employing the flowing electrolyte from one side, the concentration becomes more uniform. However, the concentration in the upper half with the side flow is more uniform than in the lower half as shown in Fig. 8b, which matches the dendrite position on the zinc electrode shown in Fig. S5 (SI). Fig. 8c shows the concentration distribution with the direct flow. No visible concentration difference is observed in the whole battery. Thus, the flow orientation design can effectively modify the zinc dendrite deposition and improve the stability of the zinc electrode. Fig. S7a and S7b (SI) give the zincate distribution with the inlet flow rate of 0.02 and 0.5 m s^{-1}, respectively. Combined with Fig. 8c, it is found that the zincate gradient around the zinc electrode surface gradually shrinks with an increase of the flow rate, but the optimized amplitude decreases when the flow rate is at a high level, as shown in Fig. 8c and Fig. S7b (SI), which means that an optimal flow rate exists to balance the cycle life and the pump work. It is worth noting that the present work is based on zinc plates

so that only an electrolyte chamber with different flow orientations are considered for preliminary investigations. For practical applications, the zinc electrode may be modified using a zinc particle-decorated three-dimensional porous electrode [39]. In such electrodes, the flow filed should be further studied and optimized, which will be reported in our subsequent work.

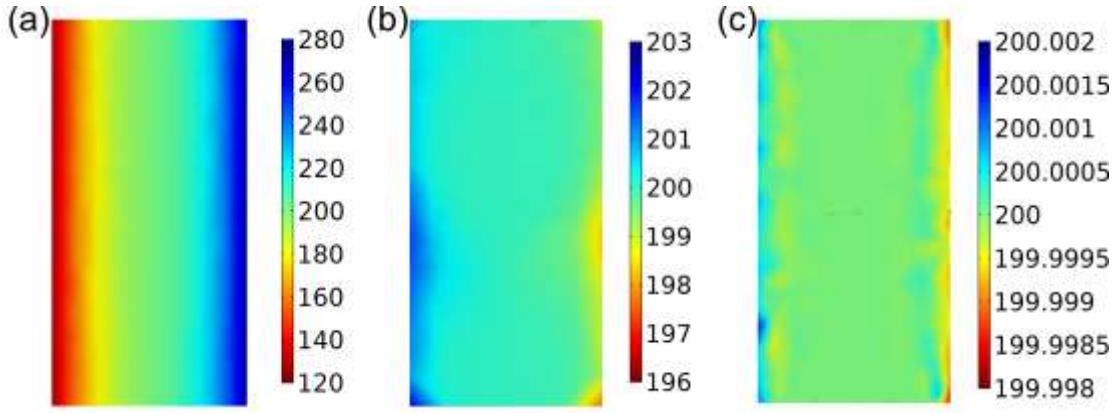

Fig. 8. Zincate ion concentration distribution of the battery profile between the negative and positive electrodes. (a) static electrolyte; (b) side-channel flowing electrolyte; (c) direct-channel flowing electrolyte.

4. Conclusions

In this work, we have conducted symmetric experiments and numerical investigations to reveal the impacts of flowing electrolyte on the cycling stability of the zinc electrode. In a static condition, the lifespan of the zinc electrode decreases with an increase of the discharge capacity, which changes from 189 to 21 h when the discharge time increases from 1 to 10 min. This is because the zincate concentration gradient around the zinc electrode increases with the time goes by, making it easier for dendrite growth. Conversely, the applied current density is positively related to the stability of the zinc electrode. The lifespan at the current density of 15 mA cm^{-2} is 250

h, much higher than that at 1 mA cm^{-2} (89 h), which is attributed to the more compact structure of deposited zinc at high current densities. In the presence of a flowing electrolyte, the dendrite growth is effectively inhibited and the lifespan of the zinc electrode is improved notably. At a low current density of 1 mA cm^{-2}, the lifespan is pulled up from 57 cycles (38 h) to 1279 cycles (853 h) when employing a flow rate of 30 rad min^{-1}. As for a high current density of 10 mA cm^{-2}, compared to the 900 cycles (60 h) in the static condition, the lifespan is also apparently improved to 4725 cycles (315 h) at a flow rate of 50 rad min^{-1}. To fully utilize the flowing electrolyte, the inlet flow orientation is changed from the side to the bottom. Consequently, the cycle times are improved to a remarkable value of 18000 cycles (1200 h), which outclasses the value of 2580 cycles (172 h) with the side flow channel. The numerical results indicate that the flowing electrolyte accelerates the transport of zincate ions and contributes to a more uniform distribution. With the implementation of the flowing electrolyte, durable secondary zinc-based batteries with low cost, high performance, and safety have extensive application prospects, especially for the large-scale energy storage grids.

Acknowledgments

P. Tan thanks the funding supports from CAS Pioneer Hundred Talents Program (KJ2090130001), USTC Research Funds of the Double First-Class Initiative (YD2090002006), Joint Laboratory for USTC and Yanchang Petroleum (ES2090130110), and USTC Tang Scholar. Z. Wu thanks the funding support from Hong Kong Scholar Program (XJ2017023). M. Ni thanks the funding support from The

Hong Kong Polytechnic University (G-YW2D) and a grant (Project Number: PolyU 152214/17E) from Research Grant Council, University Grants Committee, Hong Kong SAR.

References

[1] Y. Zeng, X. Zhang, Y. Meng, M. Yu, J. Yi, Y. Wu, X. Lu, Y. Tong, Achieving Ultrahigh Energy Density and Long Durability in a Flexible Rechargeable Quasi-Solid-State Zn–MnO_2 Battery, Adv. Mater. 29 (2017) 1700274. https://doi.org/10.1002/adma.201700274.

[2] Z. Tan, Z. Yang, X. Ni, H. Chen, R. Wen, Effects of calcium lignosulfonate on the performance of zinc-nickel battery, Electrochim. Acta 85 (2012) 554–559. https://doi.org/10.1016/j.electacta.2012.08.111.

[3] M. Senthilkumar, T.V.S.L. Satyavani, A.S. Kumar, Effect of temperature and charge stand on electrochemical performance of silver oxide-zinc cell, J. Energy Storage 6 (2016) 50–58. https://doi.org/10.1016/j.est.2016.02.008.

[4] Q. Guan, Y. Li, X. Bi, J. Yang, J. Zhou, X. Li, J. Cheng, Z. Wang, B. Wang, J. Lu, Dendrite-Free Flexible Fiber-Shaped Zn Battery with Long Cycle Life in Water and Air, Adv. Energy Mater. 9 (2019) 1901434. https://doi.org/10.1002/aenm.201901434.

[5] J. Fu, Z.P. Cano, M.G. Park, A. Yu, M. Fowler, Z. Chen, Electrically Rechargeable Zinc–Air Batteries: Progress, Challenges, and Perspectives, Adv. Mater. 29 (2017) 1604685. https://doi.org/10.1002/adma.201604685.

[6] J. Zheng, Q. Zhao, T. Tang, J. Yin, C.D. Quilty, G.D. Renderos, X. Liu, Y. Deng,

L. Wang, D.C. Bock, C. Jaye, D. Zhang, E.S. Takeuchi, K.J. Takeuchi, A.C. Marschilok, L.A. Archer, Reversible epitaxial electrodeposition of metals in battery anodes, Science 366 (2019) 645–648. https://doi.org/10.1126/science.aax6873.

[7] X. Wang, B. Xi, Z. Feng, W. Chen, H. Li, Y. Jia, J. Feng, Y. Qian, S. Xiong, Layered $(NH_4)_2V_6O_{16}\cdot 1.5H_2O$ nanobelts as a high-performance cathode for aqueous zinc-ion batteries, J. Mater. Chem. A 7 (2019) 19130–19139. https://doi.org/10.1039/c9ta05922a.

[8] Y. Li, J. Fu, C. Zhong, T. Wu, Z. Chen, W. Hu, K. Amine, J. Lu, Recent Advances in Flexible Zinc-Based Rechargeable Batteries, Adv. Energy Mater. 9 (2019) 1802605. https://doi.org/10.1002/aenm.201802605.

[9] D. Kundu, B.D. Adams, V. Duffort, S.H. Vajargah, L.F. Nazar, A high-capacity and long-life aqueous rechargeable zinc battery using a metal oxide intercalation cathode, Nat. Energy 1 (2016) 1–8. https://doi.org/10.1038/nenergy.2016.119.

[10] X. Han, X. Li, J. White, C. Zhong, Y. Deng, W. Hu, T. Ma, Metal–Air Batteries: From Static to Flow System, Adv. Energy Mater. 8 (2018) 1801396. https://doi.org/10.1002/aenm.201801396.

[11] J. Lee, S.T. Kim, R. Cao, N. Choi, M. Liu, K.T. Lee, Metal–Air Batteries with High Energy Density: Li–Air versus Zn–Air, Adv. Energy Mater. 1 (2011) 34–50. https://doi.org/10.1002/aenm.201000010.

[12] P. Pei, K. Wang, Z. Ma, Technologies for extending zinc–air battery's cyclelife: A review, Appl. Energy 128 (2014) 315–324.

https://doi.org/10.1016/j.apenergy.2014.04.095.

[13] J. Yi, P. Liang, X. Liu, K. Wu, Y. Liu, Y. Wang, Y. Xia, J. Zhang, Challenges, mitigation strategies and perspectives in development of zinc-electrode materials and fabrication for rechargeable zinc-air batteries, Energy Environ. Sci. 11 (2018) 3075–3095. https://doi.org/10.1039/c8ee01991f.

[14] S. Thomas, I.S. Cole, M. Sridhar, N. Birbilis, Revisiting zinc passivation in alkaline solutions, Electrochim. Acta 97 (2013) 192–201. https://doi.org/10.1016/j.electacta.2013.03.008.

[15] H. Kim, G. Jeong, Y.U. Kim, J.H. Kim, C.M. Park, H.J. Sohn, Metallic anodes for next generation secondary batteries, Chem. Soc. Rev. 42 (2013) 9011–9034. https://doi.org/10.1039/c3cs60177c.

[16] W. Lu, C. Xie, H. Zhang, X. Li, Inhibition of Zinc Dendrite Growth in Zinc-Based Batteries, ChemSusChem 11 (2018) 3996–4006. https://doi.org/10.1002/cssc.201801657.

[17] H. Li, C. Xu, C. Han, Y. Chen, C. Wei, B. Li, F. Kang, Enhancement on Cycle Performance of Zn Anodes by Activated Carbon Modification for Neutral Rechargeable Zinc Ion Batteries, J. Electrochem. Soc. 162 (2015) A1439–A1444. https://doi.org/10.1149/2.0141508jes.

[18] J.F. Parker, C.N. Chervin, I.R. Pala, M. Machler, M.F. Burz, J.W. Long, D.R. Rolison, Rechargeable nickel-3D zinc batteries: An energy-dense, safer alternative to lithium-ion, Science 356 (2017) 415–418. https://doi.org/10.1126/science.aak9991

[19] L.P. Wang, N.W. Li, T.S. Wang, Y.X. Yin, Y.G. Guo, C.R. Wang, Conductive graphite fiber as a stable host for zinc metal anodes, Electrochim. Acta 244 (2017) 172–177. https://doi.org/10.1016/j.electacta.2017.05.072.

[20] T.C. Adler, F.R. McLarnon, E.J. Cairns, Investigations of a New Family of Alkaline-Fluoride-Carbonate Electrolytes for Zinc/Nickel Oxide Cells, Ind. Eng. Chem. Res. 37 (1998) 3237–3241. https://doi.org/10.1021/ie9800694.

[21] J.M. Wang, L. Zhang, C. Zhang, J.Q. Zhang, Effects of bismuth ion and tetrabutylammonium bromide on the dendritic growth of zinc in alkaline zincate solutions, J. Power Sources 102 (2001) 139–143. https://doi.org/10.1016/S0378-7753(01)00789-3.

[22] H.I. Kim, H.C. Shin, SnO additive for dendritic growth suppression of electrolytic zinc, J. Alloys Compd. 645 (2015) 7–10. https://doi.org/10.1016/j.jallcom.2015.04.208.

[23] J.L. Zhu, Y.H. Zhou, C.Q. Gao, Influence of surfactants on electrochemical behavior of zinc electrodes in alkaline solution, J. Power Sources 72 (1998) 231–235. https://doi.org/10.1016/S0378-7753(97)02705-5.

[24] C.J. Lan, C.Y. Lee, T.S. Chin, Tetra-alkyl ammonium hydroxides as inhibitors of Zn dendrite in Zn-based secondary batteries, Electrochim. Acta 52 (2007) 5407–5416. https://doi.org/10.1016/j.electacta.2007.02.063.

[25] A. Bani Hashemi, G. Kasiri, F. La Mantia, The effect of polyethyleneimine as an electrolyte additive on zinc electrodeposition mechanism in aqueous zinc-ion batteries, Electrochim. Acta 258 (2017) 703–708.

https://doi.org/10.1016/j.electacta.2017.11.116.

[26] G. Garcia, E. Ventosa, W. Schuhmann, Complete Prevention of Dendrite Formation in Zn Metal Anodes by Means of Pulsed Charging Protocols, ACS Appl. Mater. Interfaces 9 (2017) 18691–18698. https://doi.org/10.1021/acsami.7b01705.

[27] F.R. McLarnon, E.J. Cairns, The secondary alkaline zinc electrode, J. Electrochem. Soc. 138 (1991) 645–664. https://doi.org/10.1149/1.2085653.

[28] Y. Ito, X. Wei, D. Desai, D. Steingart, S. Banerjee, An indicator of zinc morphology transition in flowing alkaline electrolyte, J. Power Sources 211 (2012) 119–128. https://doi.org/10.1016/j.jpowsour.2012.03.056.

[29] W. Yu, W. Shang, P. Tan, B. Chen, Z. Wu, H. Xu, Z. Shao, M. Liu, M. Ni, Toward a new generation of low cost, efficient, and durable metal–air flow batteries, J. Mater. Chem. A 7 (2019) 26116–26122. https://doi.org/10.1039/C5TA00355E.

[30] L. Zhang, J. Cheng, Y. Yang, Y. Wen, Study of zinc electrodes for single flow zinc / nickel battery application, J. Power Sources 179 (2008) 381–387. https://doi.org/10.1016/j.jpowsour.2007.12.088.

[31] X.W. Keliang Wang, Pucheng Pei, Ze Ma, Huachi Xu, Pengcheng Li, Morphology control of zinc regeneration for zinc-air fuel cell and battery, J. Power Sources 271 (2014) 65–75. https://doi.org/10.1016/j.jpowsour.2014.07.182.

[32] B. Li, J. Quan, A. Loh, J. Chai, Y. Chen, C. Tan, X. Ge, T.S.A. Hor, Z. Liu, H.

Zhang, Y. Zong, A Robust Hybrid Zn-Battery with Ultralong Cycle Life, Nano Lett. 17 (2017) 156–163. https://doi.org/10.1021/acs.nanolett.6b03691.

[33] C.Y. Chen, K. Matsumoto, K. Kubota, R. Hagiwara, Q. Xu, A Room-Temperature Molten Hydrate Electrolyte for Rechargeable Zinc–Air Batteries, Adv. Energy Mater. 9 (2019) 1900196. https://doi.org/10.1002/aenm.201900196.

[34] P. Pei, S. Huang, D. Chen, Y. Li, Z. Wu, P. Ren, K. Wang, X. Jia, A high-energy-density and long-stable-performance zinc-air fuel cell system, Appl. Energy 241 (2019) 124–129. https://doi.org/10.1016/j.apenergy.2019.03.004.

[35] K. Wang, P. Pei, Y. Wang, C. Liao, W. Wang, S. Huang, Advanced rechargeable zinc-air battery with parameter optimization, Appl. Energy 225 (2018) 848–856. https://doi.org/10.1016/j.apenergy.2018.05.071.

[36] J. Cheng, L. Zhang, Y.S. Yang, Y.H. Wen, G.P. Cao, X.D. Wang, Preliminary study of single flow zinc-nickel battery, Electrochem. Commun. 9 (2007) 2639–2642. https://doi.org/10.1016/j.elecom.2007.08.016.

[37] Y. Jiang, Y.P. Deng, J. Fu, D.U. Lee, R. Liang, Z.P. Cano, Y. Liu, Z. Bai, S. Hwang, L. Yang, D. Su, W. Chu, Z. Chen, Interpenetrating Triphase Cobalt-Based Nanocomposites as Efficient Bifunctional Oxygen Electrocatalysts for Long-Lasting Rechargeable Zn–Air Batteries, Adv. Energy Mater. 8 (2018) 2018. https://doi.org/10.1002/aenm.201702900.

[38] S.S. Shinde, C.H. Lee, J.Y. Jung, N.K. Wagh, S.H. Kim, D.H. Kim, C. Lin, S.U. Lee, J.H. Lee, Unveiling dual-linkage 3D hexaiminobenzene metal-organic

frameworks towards long-lasting advanced reversible Zn-air batteries, Energy Environ. Sci. 12 (2019) 727–738. https://doi.org/10.1039/c8ee02679c.

[39] A.L. Zhu, D.P. Wilkinson, X. Zhang, Y. Xing, A.G. Rozhin, S.A. Kulinich, Zinc regeneration in rechargeable zinc-air fuel cells — A review, J. Energy Storage 8 (2016) 35–50. https://doi.org/10.1016/j.est.2016.09.007.